Mini-Beta Lattice for the Femto-Second X-Ray Source at the Advanced Light Source [1]

Y. Wu, H. Nishimura, D. S. Robin, A. A. Zholents
Lawrence Berkeley National Laboratory, 1 Cyclotron Road, Berkeley, CA 94720, USA
E. Forest
High Energy Accelerator Research Organization, 1-1 Oho, Tsukuba, Ibaraki 305-0810, Japan

Abstract

After generating the first femto-second X-ray pulses at the Advanced Light Source (ALS), it becomes critical to improve the flux of this femto-second source for the user experiments. A narrow-gap in-vacuum undulator has been proposed to be installed in one of the ALS straight sections. To realize the optimal performance of this undulator, a straight section lattice with a mini vertical beta function has been designed. Separation of electrons has been achieved by generating a sizable vertical dispersion via a local dispersion bump and a closed orbit bump. Particle tracking study shows that the modified ALS lattice for the femto-second x-ray source has an adequate dynamic aperture.

[1]Work supported by the Director, Office of Energy Research, Office of Basic Energy Sciences, Material Sciences Division, U.S. Department of Energy, under Contract No. DE-AC03-76SF00098.

1 Introduction

A source of femto-second x-ray pulses had been recently commissioning at the Advanced Light Source (ALS) [1]. This source utilizes the technique where an ultra-short laser pulse is used to modulate the energy of electrons within a 100-femtosecond slice of the stored 30-picosecond electron bunch. The energy-modulated electrons are spatially separated from the main electron bunch by horizontal dispersion and are used to generate 300-femtosecond synchrotron radiation pulses at a bend-magnet beamline. For a good signal-to-background ratio it is important that the number of electrons that are displaced into the beam tail from the beam core is much larger than the existing population of electrons in the beam tail.

At present we are considering using an undulator rather than a bend magnet as a high flux source of femto-second x-rays. Lattice modifications have been studied to optimize the performance of this new source.

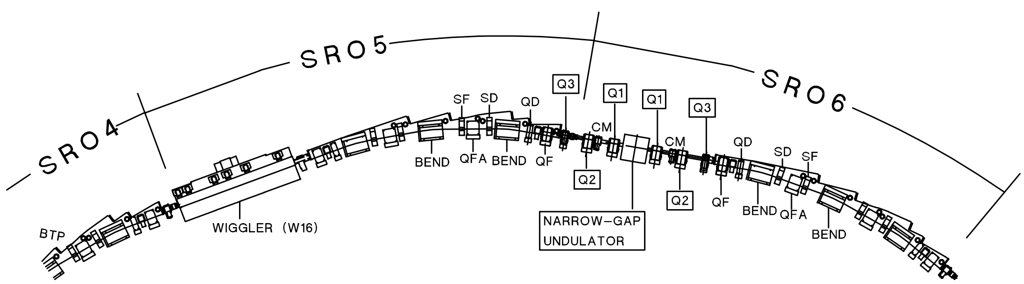

Figure 1: The layout of the ALS sector 5 and sector 6 with the wiggler magnet and the narrow-gap in-vacuum undulator. Three pairs of extra quadrupoles (Q1, Q2, Q3) are required to reduce the vertical beta function and preserve the beam dynamics.

The optimal performance of the ring with the narrow-gap undulator can be achieved by providing a small vertical beta function at the center of the undulator. A small vertical beta function provides a better match between the electron beam and x-ray beam in the undulator and helps preserve the available vertical physical aperture of the ring. In addition, a sizeable transverse η-function at the location of the narrow-gap undulator or in the neighboring wiggler is necessary to separate the energy modulated electrons from the beam core.

An effective dispersion function describing the off-energy trajectory at the center of the undulator can be defined as follows,

$$(\eta_2)_{\mathrm{eff}} = \eta_2 - (\sqrt{\frac{\beta_2}{\beta_1}} \cos\Delta\phi \; \eta_1 + \sqrt{\beta_2\beta_1} \sin\Delta\phi \; \eta_1'), \tag{1}$$

where $\alpha_1 = \alpha_2 = 0$ at the centers of the wiggler and undulator, η_1 and η_1' are dispersion functions at the center of the wiggler, η_2 is the dispersion function at the center of the undulator, and $\Delta\phi$ is the phase advance between the two centers. For a given amplitude of the relative energy modulation of electrons, $\Delta E/E_0$, the transverse separation of these electrons from the beam core is,

$$\frac{\Delta z}{\sigma_z} = \frac{\frac{\Delta E}{E_0}\,(\eta_2)_{\mathrm{eff}}}{\sqrt{\epsilon_z\beta_z + \sigma_E^2\eta_2^2}}, \tag{2}$$

where $z = x, y$ stands for one of the transverse planes, σ_z is the transverse beam size, ϵ_z, β_z are the transverse emittance and beta function, σ_E is the energy spread of the beam. It is apparent that a much smaller vertical emittance would allow us to use a smaller vertical dispersion to achieve the same amount relative separation. Let us also point out that for a given $(\eta_2)_{\mathrm{eff}}$, the dispersion generated at the wiggler has advantage over that in the undulator for the transverse beam size depends on the dispersion function.

A good signal-to-noise ratio for the femto-second x-ray radiation can be achieved by providing adequate transverse separation of the energy modulated electrons from the electron beam core [2]. A separation of 5σ is desirable at the center of the undulator where $\beta_y = 0.5$ m. This can be achieved by a laser induced energy modulation of ~ 9 MeV (readily available in the current system) and an effective vertical dispersion of $(\eta_2)_{\mathrm{eff}} \approx 8.5$ mm, assuming a two percent emittance coupling, i.e. $\epsilon_y = 10^{-10}$ m-rad.

The narrow-gap undulator source also means a much reduced vertical physical aperture.

A 5 mm undulator gap is almost a factor of three smaller than the smallest magnetic gap (14 mm) and is nearly a factor of two smaller than the narrowest vacuum chamber (9 mm) that presently exists in the ALS ring. One needs to be concerned with the potential negative impact on the ring performance due to such a significant reduction in aperture, namely the injection efficiency and lifetime. In particular, the inclusion of this device should not significantly change the single particle beam dynamics and a minimal of ± 10 mm horizontal dynamic aperture should remain for injection.

2 Single Particle Beam Dynamics

The ALS ring consists of 12 sectors, the 16-cm period wiggler (W16) is located in straight 5 and the narrow-gap undulator will be located in straight 6 (see Fig. 1). To accommodate the narrow-gap undulator, the vertical β-function of straight 6 needs to be lowered from the nominal value of 4.0 m to 0.5 m. Therefore, the lattice periodicity breaking is inevitable due to this lattice modification in one of the twelve otherwise identical sectors in the ALS ring. If one is not careful in the design of the narrow-gap straight, the strong nonlinearities in the lattice become unbalanced to yield a significant dynamic aperture reduction as observed in our first simple mini-beta lattice design using two extra quadrupole families.

On the other hand, it is well known that the on-momentum single particle dynamics is unaffected if a portion of linear lattice is modified in such a way that a multiply of 2π phase advance ($2\,n\,\pi$, $n =$ integer) is added to either transverse plane while keeping this modified portion matched to the rest of the ring lattice. However, it is impractical to implement such a large phase advance change in the extremely short ALS straight. Noticing that the ALS ring employs only the magnets with a mid-plane symmetry (normal dipoles, quadrupoles, and sextupoles) in its baseline lattice, we find that the vertical phase advance of any part of the linear ring lattice can be increased by π without affecting the on-momentum single particle dynamics.

Let us prove this. Suppose that $\mathcal{N} = \exp(:g(\mathbf{z}):)$ is the one-turn Lie map for the unmodified ring with the mid-plane symmetry, where $g(\mathbf{z})$ is the one-turn Lie operator and $\mathbf{z} = \{x, p_x, y, p_y\}$ is the 4D phase space variable. Since this ring consists of only magnets with the mid-plane symmetry, $g(\mathbf{z})$ is an even function of y and p_y, which yields,

$$\mathcal{N}(x, p_x, -y, -p_y) = \mathcal{N}(x, p_x, y, p_y). \tag{3}$$

Now we add a matched section to the linear lattice to alter its phase advances with $\Delta\phi_x = 2m\,\pi$ and $\Delta\phi_y = (2n+1)\,\pi$, where $m, n =$ integer. The Lie map for this addition, $\mathcal{R}(\mathbf{z})$, satisfies:

$$\mathcal{R}\,x = x, \quad \mathcal{R}\,p_x = p_x, \quad \mathcal{R}\,y = -y, \quad \mathcal{R}\,p_y = -p_y, \qquad \text{and} \qquad \mathcal{R}^{-1} = \mathcal{R}. \tag{4}$$

Writing the modified one-turn map, $\mathcal{M} = \mathcal{N}\mathcal{R}$, we find for two turns:

$$\mathcal{M}^2 = \mathcal{N}\,\mathcal{R}\,\mathcal{N}\,\mathcal{R} = \mathcal{N}\,\exp(:\mathcal{R}\,g(\mathbf{z}):) = \mathcal{N}\,\exp(:g(\mathbf{Rz}):) = \mathcal{N}\,\exp(:g(\mathbf{z}):) = \mathcal{N}^2. \tag{5}$$

Thus it results in exactly the same two-turn 4D map as for the original ring. This proves the theorem.

A particular application of this idea is for the linear lattice modification to gain a π phase advance increase in the vertical plane while keeping the horizontal phase advance unchanged, i.e. $\Delta\phi_x = 0$, and $\Delta\phi_y = \pi$. Such a solution is referred as the π-trick. It is worth pointing out that by adding extra focusing elements, a slight increase in sextupole strengths will be needed in the modified ring to properly compensate the chromaticity. This will have a slight impact on the dynamic aperture.

Applying the π-trick, we designed two mini-beta lattices for the cases when the wiggler is either open or closed. A symmetric mini-beta lattice using three pairs of additional quadrupoles in the sector 6 was designed for the case when the wiggler is open (see Fig. 2). However, during normal wiggler operation, two defocusing quadrupoles in sectors 4 and

6 are used to compensate the vertical beta-beating induced by the wiggler focusing. To compensate for this effect, a slightly asymmetric mini-beta lattice with six independently powered quadrupoles was also designed. We performed particle tracking for both mini-beta lattices without errors to determine the available bare lattice dynamic apertures. The results are compared with the standard ALS lattices. Fig. 3 shows that the on-momentum dynamic apertures of the ALS lattice remains the same after the mini-beta straight is created regardless of whether the wiggler is open or closed. These results illustrate the effectiveness of the π-trick. Note that the wiggler compensation in the unmodified ALS ring breaks the twelve-fold symmetry of the lattice to a certain degree, which has already resulted in a reduced dynamic aperture (comparing Fig. 3.(a) and Fig. 3.(b)).

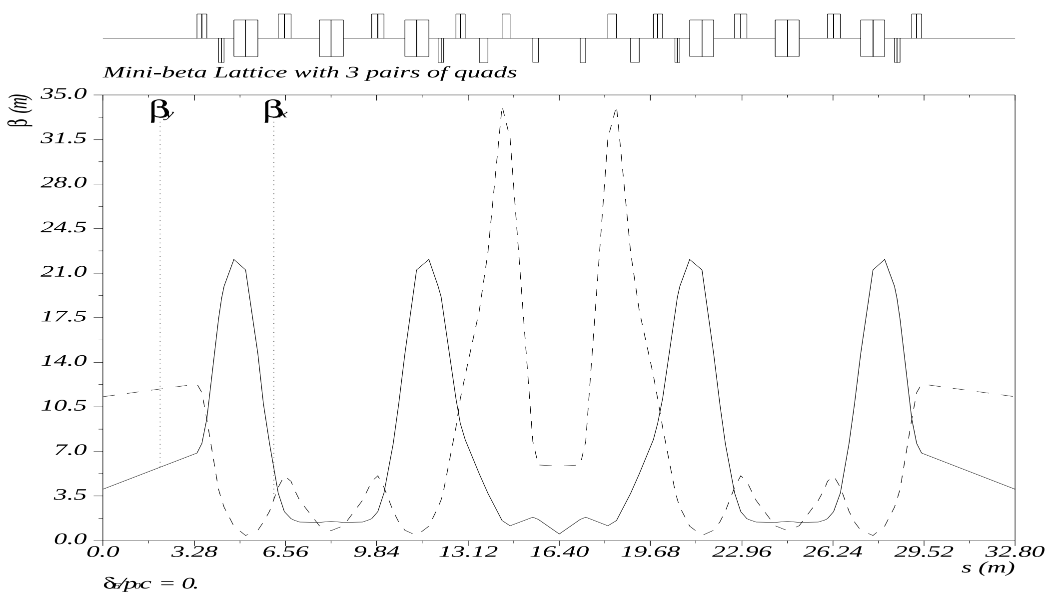

Figure 2: Symmetric mini-beta lattice with modified phase advances: $\Delta\phi_x = 0, \Delta\phi_y = \pi$.

3 Generation of Vertical Dispersion

Two methods have been studied to generate the vertical dispersion in either the wiggler or narrow-gap undulator. The first method creates a vertical η-bump by coupling the horizontal dispersion into the vertical plane. The second method generates a vertical η-

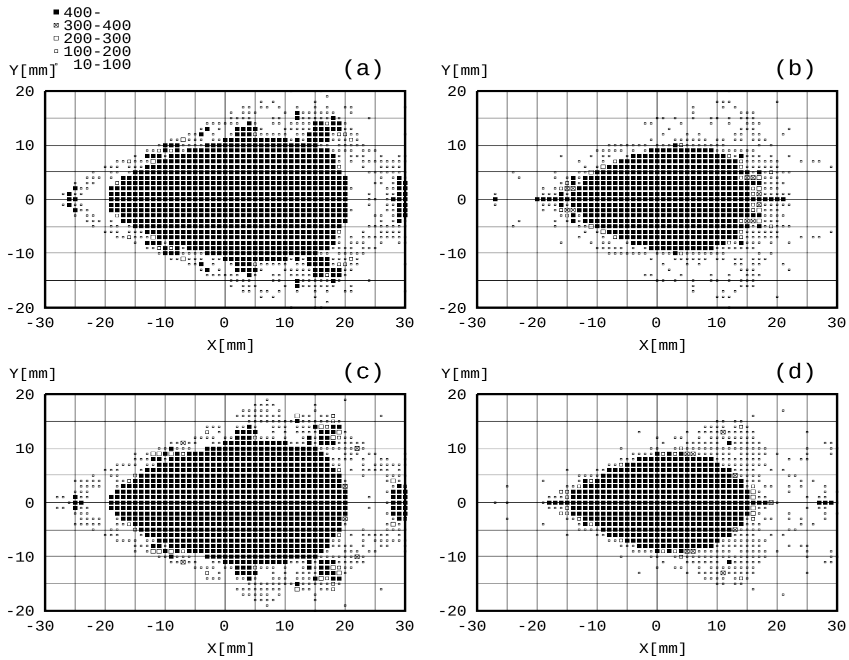

Figure 3: Dynamic apertures at the center of the regular straight ($\beta_x = 11$ m and $\beta_y = 4$ m) for the ALS bare lattice with or without the mini-beta modification. Particles survived after more than 400 turns of tracking are considered to be stable. (a) ALS lattice with the wiggler open; (b) ALS lattice with the wiggler closed; (c) modified mini-beta lattice with the wiggler open; (d) modified mini-beta lattice with the wiggler closed.

wave using a local vertical orbit bump.

3.1 Eta Bump by Coupling

At the ALS, sextupoles are equipped with the coils producing skew gradient of the magnetic field. Skew quadrupoles can be used to transform horizontal dispersion into the vertical plane. A skew quadrupole kicks the horizontal dispersion into the vertical plan in the same way that a corrector magnet steers a closed orbit distortion around the ring. Turning on a skew quadrupole at the location s_0 with the horizontal eta function $\eta_x(s_0)$, a vertical η-function wave will be produced,

$$\eta_y(s) = \frac{K}{2\sin(\pi\nu_y)}\,\eta_x(s_0)\sqrt{\beta_y(s)\beta_y(s_0)}\,\cos(\phi_y(s_0) - \pi\nu_y), \tag{6}$$

where K is the normalized strength of the skew gradient, ϕ_y is the vertical phase advance, and ν_y is the vertical tune. A symmetric local vertical η-bump can be created using two pairs of skew quadrupoles in a part of lattice with mirror symmetry. However, due to the global coupling, some combinations of the skews would result in unacceptably large vertical emittances.

Eight skew quadrupoles in the neighboring arc sections are available for generating the vertical η-bump around the wiggler. A total of six different symmetric four-skew quadrupole bump combinations have been studied in their effectiveness in generating the vertical η-bump and in their contributions to the emittance coupling. However, in practice, the skew gradient in the ALS sextupoles are limited to a maximum value of $K = 0.0237$ at 1.9 GeV. By limiting a total vertical emittance coupling to 1%, an optimal combination of the vertical η-bumps was found to create a $\eta_y = 17$ mm at the center of the wiggler, which corresponding to an effective $(\eta_y)_{\text{eff}} = 6.5$ mm at the center of the narrow-gap undulator. An ever larger vertical η-bump can be readily realized if the skew windings in sextupole magnets can be powered at higher values. In addition, individual skew quadrupoles can be located at optimized locations to facilitate the generation of the η-bump while controlling the emittance coupling.

In Fig. 4(a), we plot the local η-bump around the wiggler with the wiggler closed. The dynamic aperture of this lattice is shown in Fig. 4(b). The reduction in the dynamic aperture (as compared with Fig. 3.(b)), is caused again by further periodicity breaking due to the coupling. Nevertheless, the remaining dynamic aperture is still adequate for injection and good beam lifetime.

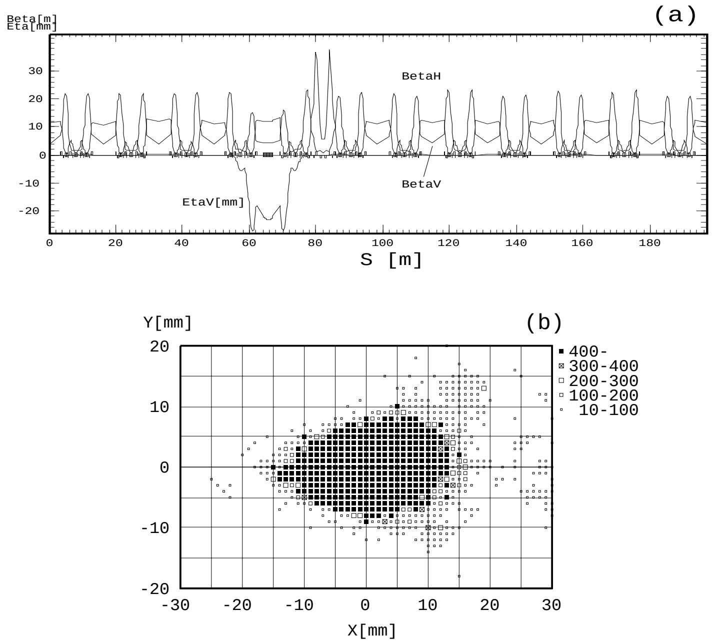

Figure 4: A mini-beta lattice with a vertical η-bump of 17 mm at the center of the wiggler ($\eta_{\text{eff}} = 6.5$ mm). (a) beta functions and vertical eta bump; (b) dynamic aperture tracking.

3.2 Eta Wave by Local Orbit Bump

Eta-function can also be generated by the closed-orbit. The following formula describes the eta-function produced by an angle kick $\theta(s) = \theta_0(1 - \delta)$ at location s:

$$\begin{pmatrix} \eta \\ \eta' \end{pmatrix} = -(I - M)^{-1} \cdot \left(\begin{pmatrix} 0 \\ \theta_0(s) \end{pmatrix} - \left.\frac{dM}{d\delta}\right|_{\delta=0} \cdot \begin{pmatrix} x_{\text{co}} \\ x'_{\text{co}} \end{pmatrix} \right), \tag{7}$$

where, M is the on-turn matrix, x_{co} and x'_{co} is the orbit at s, and δ is the momentum deviation of the particle. It is apparent that arbitrary closed orbit will result in uncontrolled eta-wave around the ring. On the other hand a closed orbit bump can be utilized to control the eta function at the certain locations in the ring.

In fact, the present vertical closed-orbit in the ALS produces a measured ± 2 mm vertical η-function distributed around the ring, which could account for some undesirable η'_y at the center of the narrow-gap undulator. To correct and control this unwanted η'_y in the undulator, a localized vertical orbit bump around the undulator can be used. In addition it can enhance the vertical separation of the energy modulated electrons. In Fig. 5, a 0.4 mm vertical orbit bump at the center of the narrow-gap undulator yields an effective η_y = 3.6 mm at the same location. Since the orbit bump is mostly located in the linear lattice, nonlinearity of the lattice is almost unperturbed. Particle tracking confirms that the dynamic aperture is unchanged with this local orbit bump.

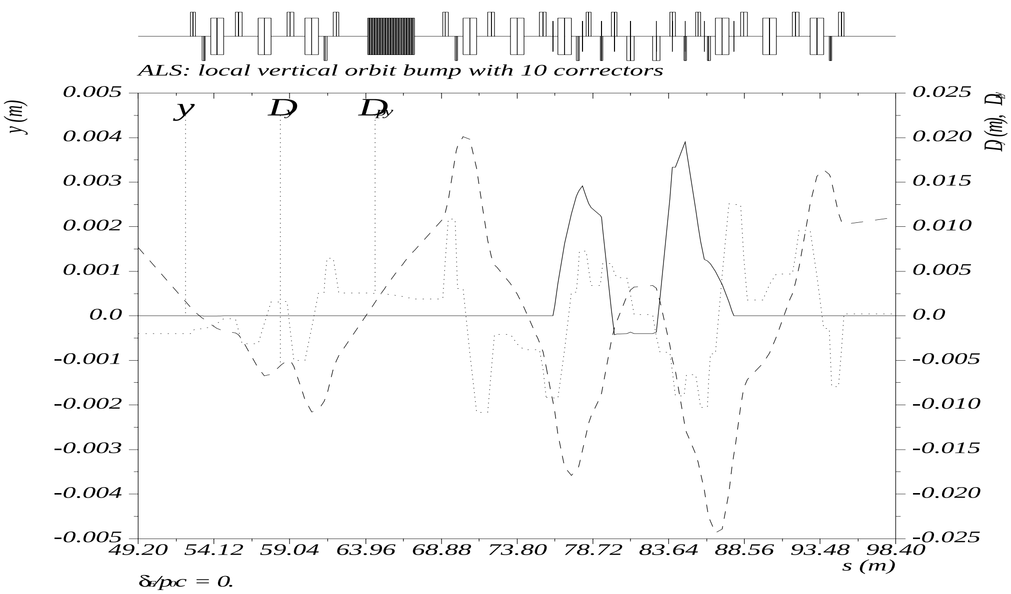

Figure 5: Vertical orbit bump and η-wave around the ring. The solid line is the vertical orbit and the dashed line is η_y.

4 Mini-Beta Lattice With Eta Bumps

By combining the two different methods to generate vertical η-function, we assembled a complete mini-beta lattice to produce an effective η_y about 10 mm at the center of the narrow-gap undulator (see Fig. 6.(a)). Particle tracking indicated that this lattice has an adequate dynamic aperture (see Fig. 6.(b)).

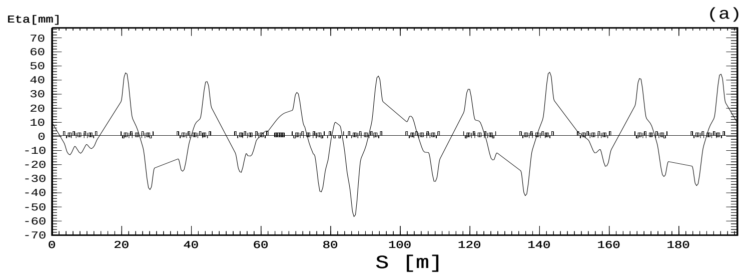

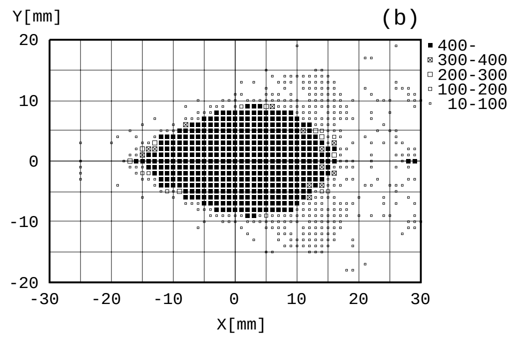

Figure 6: The vertical η-wave and dynamic aperture for a lattice with $(\eta_y)_{\text{eff}} = 10$ mm. (a) η-function generated by both the η-bump and vertical local orbit; (b) dynamic aperture for the lattice.

5 Conclusion

A mini-beta lattice ($\beta_y = 0.5$ m) has been designed to accommodate the narrow-gap undulator for the future femto-second x-ray source. We developed a novel technique to restore the single particle nonlinear dynamics in the ALS by increasing the vertical betatron phase advance by π in the mini-beta lattice while keeping the horizontal phase advance unchanged. This technique allows practical lattice modifications for light source rings like the ALS to accommodate special insertion devices such as narrow-gap undulators. We investigated two different methods to generate the vertical η-function by either coupling the horizontal dispersion into the vertical plane using skew quadrupoles or by a local vertical orbit bump. A complete lattice solution with an effective $\eta_y = 10$ mm at the center of the narrow-gap undulator has been found with adequate dynamic aperture for electron beam injection and lifetime.

Acknowledgments

The authors would like to thank Alan Jackson at LBNL for initial suggestion of the π-trick, and Tom Henderson at LBNL for laying out the mechanical design of the mini-beta straight lattice.

References

[1] R.W.Schoenlein et.al., *Generation of Femtosecond Pulses of Synchrotron Radiation*, Science, pp. 2237–2240, March 24, 2000.

[2] A. Zholents, W. Decking, *Non-Gaussian Tails at the Advanced Light Source*, LBNL-45392, to be presented at EPAC 2000.